Community structure and feeding ecology of meiofauna associated with methane seepage at the Darwin mud volcano (Gulf of Cádiz)

Ellen Pape[1,*], Tania Nara Bezerra[1], Heleen Vanneste[2], Katja Heeschen[2], Leon Moodley[3], Frederic Leroux[4], Peter van Breugel[3] & Ann Vanreusel[1]

[1] Marine Biology Section, Biology department, Ghent University, Krijgslaan 281/S8, 9000 Gent, Belgium

[2] National Oceanography Centre Southampton, University of Southampton, Waterfront Campus, European Way, Southampton, SO14 3ZH UK

[3] NIOO-CEME, Workgroup of Ecosystem studies, Korringaweg 7, 4401 NT Yerseke, the Netherlands

[4] EMAT, University of Antwerp, Groenenborgerlaan 171, B-2020 Antwerpen, Belgium

* Corresponding author, Ellen.Pape@Ugent.be

ABSTRACT: We sampled the Darwin mud volcano (MV) for meiofaunal community and trophic structure in relation to pore-water geochemistry along a 10-m transect from a seep site on the rim of the crater towards the MV slope. Pore-water profiles indicated considerable variation in upward methane (CH_4) flow among sediment cores taken along the transect, with highest flux in the seep sediment core, gradually decreasing along the transect, to no CH_4 flux in the core taken at a 5 m distance. Low sulphate concentrations and high levels of total alkalinity and sulphide (H_2S) suggested that anaerobic oxidation of methane (AOM) occurred close to the sediment surface in the seep sediment core. High H_2S

levels had a genus and species-specific impact on meiofaunal densities. Nematode genus composition varied gradually between sediment cores, with the genus *Sabatieria* dominating almost all sediment cores. However, genus diversity increased with increasing distance from the seep site. These limited data suggest that the community structure of seep meiofauna is highly dependent on local (a)biotic habitat characteristics, and a typical seep meiofauna community cannot be delineated. Stable isotope values suggested the nematode diet up to 10 m from the seep site included thiotrophic carbon. The thicker hemipelagic sediment layer (photosynthetic carbon), the increased trophic diversity, and the heavier nematode $\delta^{13}C$ farther from the seep site suggest a decrease in thiotrophy and an increase in photosynthetic carbon in the nematode diet.

Key words: cold seeps; diversity; stable isotopes; nematodes; diet

---

INTRODUCTION

Mud volcanoes (MVs), geological structures driven by fluid flow, are characterized by a high patchiness of biochemical and physical characteristics. Fluid flow rates, pore-water concentrations of hydrogen sulphide (H_2S) and methane (CH_4), and the thickness of the hemipelagic sediment veneer, on top of the reduced sediments, can change rapidly over short distances (m - cm) (Levin et al. 2003). The heterogeneity in these properties is the main parameter driving the distribution of macro- and megafauna at seeps (Levin 2005), resulting in patches of tubeworm clusters, mussels or clams, and bacterial mats or bare reduced sediments. Meiofauna can also vary on a scale of meters in taxonomic composition and biodiversity in relation to sediment biogeochemistry (Van Gaever et al. 2009c).

There is no consistent meiofaunal response to seep conditions. Meiofaunal densities at different deep-sea seeps are higher (Olu-Le Roy et al. 1997, Van Gaever et al. 2006) or similar (Shirayama & Ohta 1990) compared to non-seep sediments. In seep environments, nematodes usually are the predominant metazoans, although sometimes copepods dominate (Van Gaever et al. 2006). Generally, deep-sea nematodes are characterized by high local diversity (Lambshead & Boucher 2003). Cold seeps, however, exhibit substantially reduced species diversity, harbouring only a few dominant species (Levin 2005, Vanreusel et al. 2010). The low diversity in these habitats has been attributed to the harsh abiotic conditions, created by the high H_2S and low oxygen levels (Levin 2005).

Besides high biogeochemical and physical heterogeneity, seeps differ from most deep-sea environments in the local production of organic matter through chemosynthesis. Consequently, possible food sources for seep fauna, including meiobenthos, are (1) organic matter derived from symbiotic chemoautotrophic bacteria, and (2) free-living chemoautotrophic bacteria, in addition to (3) the photosynthetic organic matter, delivered to all deep-sea habitats. Studies on the diet of seep meiofauna are few. Both Van Gaever *et al.* (2006, 2009b) and Spies & DesMarais (1983) found seep nematodes to be feeding on free-living sulphur-oxidising bacteria. To date, there is no evidence of symbioses between nematodes and chemosynthetic bacteria at deep-sea seeps (Vanreusel et al. 2010), and observations of symbionts associated with seep nematodes are restricted to shallow waters (Dando et al. 1991, Ott et al. 2004).

This study examined the community structure and feeding ecology of the meiofauna, with a focus on nematodes, at a MV in the Gulf of Cádiz, which we then related to geochemical gradients along a 10-m transect going from a seep site towards nearby

hemipelagic surface sediments, and 2 sites farther away from seep influence. This study differs from previous analyses on seep meiofauna, because it concerns isolated seep sediments on a low-activity MV. We addressed the following questions:

- Does pore-water composition influence horizontal and vertical distribution of meiofauna on a small scale?
- Are the seep sediments colonized by a specialized community that differs from the hemipelagic sediments in density, biomass and taxonomic composition (genera and species)?
- What is the nematode diet inferred from stable isotope analyses and buccal morphology? Do seep conditions influence nematode trophic diversity?

MATERIALS AND METHODS

Study area. The Gulf of Cádiz (34°- 37°15' N, 9° - 6°45' W) is a tectonically active region west of the Strait of Gibraltar, encompassing the boundary between the European and African plate. It is one of the largest cold-seep areas on the European margins with over 30 MVs between 200 and 4000 m deep (Pinheiro et al. 2003, Somoza et al. 2003, Van Rensbergen et al. 2005).

The summit (1100 m depth) of the Darwin MV (35°23.51' N 7°11.48'W; Fig. 1A) is covered with a large, fractured carbonate crust. At the time of sampling, countless, but mostly empty, *Bathymodiolus mauritanicus* shells covered the MV top (Genio et al. 2008). Living specimens were only present in small clumps along cracks in the crust. When disturbed by the ROV temperature probe, a small area of dark-coloured sediment (± 100 cm^2), from here on referred to as "seep site", emitted gas. Small carbonate blocks and white sediments, indicative of bacterial activity, which covered hard substrate, surrounded the

seep site (Vanreusel et al. 2009). No dense aggregations of living chemosynthetic megafauna were associated with the seep sediments or 2 m away. At the MV centre, non-chemosynthetic megafauna comprised scavenging crabs, corals and stylasterine corals, attached to the carbonate crust.

Sampling strategy. Sediment cores were collected during the JC10 expedition to the Gulf of Cádiz in May 2007 onboard the RRS *James Cook* (Table 1). We were unable to collect replicate samples because of the high heterogeneity of the habitat and the small size of the seep site. However, this study is the first to identify potential interactions between seep meiofauna and pore-water geochemistry measured at such a small spatial scale. Furthermore, no meiofauna data were available from the Gulf of Cádiz so far, although it forms an important faunal cross road between the Mediterranean and the Atlantic.

Using ROV Isis, we collected 2 push cores (PUCs, 25.5 cm^2) at each of the 4 sites along a 10-m transect between the seep site and an area with a considerably thicker hemipelagic sediment layer (Fig. 1; Table 1). One PUC was taken with a core-liner, with openings every 2 cm, to extract pore-water using Rhizons (Seeberg-Elverfeldt et al. 2005). These pore-waters were sub-sampled on board for nutrient and anion analyses. Subsequently, we sliced the top 10 cm of this core into 1-cm sections and fixed them in 4% formaldehyde for meiofaunal community analysis. The 2^{nd} PUC was sub-sampled for CH_4 and porosity analyses, and we stored the remaining sediment in 2-cm slices at -30°C for stable isotope analysis. Besides the 10-m transect, we sampled 2 sites at ~ 100 (on the MV) and ~ 1100 m from the seep site (off the MV) with a megacorer (75.4 cm^2). These samples were exclusively analyzed for community structure.

Pore-water geochemical analyses. Total alkalinity (TA) and hydrogen sulphide (H_2S) were measured immediately after pore-water extraction; TA by titrating against 0.05 M HCl while bubbling nitrogen through the sample (Ivanenkov & Lyakhin 1978) and H_2S using standard photometric procedures (Grasshoff et al. 1999) adapted for pore-waters with high (≅ mM) H_2S levels. Concentrations of all other species were analyzed at the National Oceanography Centre Southampton (NOCS). Sulphate (SO_4^{2-}) was measured by ion chromatography (Dionex ICS2500), with reproducibility (determined by repeat analysis of a seawater standard as well as single anion standards) >1.5%. We measured dissolved CH_4 in sediment samples taken immediately after opening the cores using the headspace vial method (Reeburgh 2007). An aliquot of sediment (≅ 3 cm^3) was withdrawn, placed in a glass vial, and 5 ml of 1M NaOH was added to prevent further microbial activity (Hoehler et al. 2000). The vial was crimped shut, and the sample shaken vigorously to release the gases. CH_4 concentration in the headspace was determined by gas chromatography (Agilent 6850) at the NOCS. These headspace CH_4 measurements were then converted to dissolved CH_4 concentrations following Hoehler et al. (2000). Depressurization and warming of the cores during sediment retrieval is likely to have led to degassing, so concentrations of CH_4 (which is generally oversaturated in pore-waters) and H_2S, to a lesser extent, represent minimum values. Therefore, profiles were compared relative to one another, rather than to measurements in other studies.

Meiofaunal community analysis. We washed the formaldehyde-fixed samples over a 32-µm mesh sieve and extracted the meiofauna from the sediment by Ludox centrifugation (Heip et al. 1985). Meiofauna was then sorted, enumerated and identified at coarse taxonomic level. From each slice, ± 100 nematodes were identified to genus level. *Sabatieria*, the dominant genus in all cores but one, was identified to species. Additionally,

we measured length (µm) and maximal width (µm) for each nematode from the top 0-5 cm, to estimate individual biomass using Andrassy's formula (Andrassy 1956) for wet body weight (wwt), adjusted for the specific gravity of marine nematodes (i.e. 1.13 g cm^{-3}; µg wwt = L x W^2/1 500 000). C weight was calculated as 12.4 % of wet weight (Jensen 1984).

Stable isotope analysis. Nematodes from the top 6 cm of each core were hand-picked for $\delta^{13}C$ and $\delta^{15}N$ analysis. *Desmodora* (n = 50) and *Sabatieria* (n = 50) were picked separately, and the remaining genera were pooled to determine the "Mix" isotope value (n = 100). When not sufficiently abundant, *Desmodora* and/or *Sabatieria* were included in the "Mix" sample. Nematodes were rinsed with 2 µm filtered Milli-Q water, and then transferred to Milli-Q water in pre-combusted (550°C, 3 h) silver cups. After elutriation, nematodes were dried overnight at 60°C. Subsequently, we acidified samples and blanks in a desiccator containing 5 % HCl. Isotope signatures were measured on an EA-IRMS, a Flash EA 1112 coupled to a DeltaV advantage IRMS (Thermo Electron Instruments) with a single low volume oxidation/reduction reactor (Carman & Fry 2002). Samples were calibrated against VPDB and N_2-Air with standards USGS40 and USGS41 (Qi et al. 2003) and all measurements were corrected for blanks. Isotope values were expressed in δ notation with respect to VPDB ($\delta^{13}C$) and air ($\delta^{15}N$): δX (‰) = $[(R_{sample}-R_{standard})-1] \times 10^3$, where X is ^{13}C or ^{15}N and R is the isotope ratio (Post 2002).

Transmission electron microscopy (TEM) and scanning transmission electron microscopy energy dispersive x-ray (STEM-EDX) analysis. *Sabatieria* and *Desmodora*, from the seep sediment core, were imaged with TEM to check for symbionts or visible S detoxification structures. Subsequently, we conducted STEM-EDX analysis to determine the

158 chemical composition of internal structures. Nematodes were handled following Van Gaever
159 et al. (2009b).

160 **Data analysis.** Individual nematode size measurements (length, width, length/width and
161 biomass) were compared among cores using Krukal-Wallis tests, followed by nonparametric
162 pairwise comparisons using Behrens-Fisher tests with the R package npmc (Munzel &
163 Hothorn 2001, Helms & Munzel 2008). Nematode size measurements were averaged per
164 core and depth layer as geometric means corrected for data skewness (Middelburg et al.
165 1997, Soetaert et al. 2009). We performed multi-dimensional scaling (MDS) analysis on
166 standardized nematode genus abundances to compare genus composition between cores.
167 Diversity indices were Ln ($\log_e$)-transformed to highlight differences. We examined feeding
168 ecology based on (1) $\delta^{13}C$ and $\delta^{15}N$ of *Desmodora*, *Sabatieria* and "Mix"; and (2) buccal
169 morphology of all genera following the classification of Wieser (1952), which assigns genera
170 to one of 4 feeding types: selective deposit-feeder (1A), non-selective deposit-feeder (1B),
171 epistrate feeder (2A) and predator/scavenger (2B). Isotope signatures were compared
172 between *Sabatieria*, *Desmodora* and "Mix" using 1-way ANOVA, followed by post-hoc Tukey
173 HSD tests. Trophic diversity was computed as the reciprocal of the trophic index (Heip et al.
174 1985). Spearman-rank correlations were computed between distance from the seep site and
175 (1) genus diversity indices, (2) trophic diversity, and (3) stable isotope signatures. We
176 performed univariate statistical analyses using R (R Development Core Team 2010), and
177 multivariate analyses and computation of diversity indices in Primer v6 (Clarke & Gorley
178 2006).

179 **RESULTS**

180 **Pore-water geochemistry**

Fig. 2 shows concentration-depth profiles for H_2S, SO_4^{2-}, CH_4 and TA in pore-water from all cores. From the 4 cores, only the seep sediment core showed a clear decrease in SO_4^{2-} with depth, accompanied by a peak in H_2S (up to 22 mM) and an increase in CH_4 and TA as high as 1000 µM and 33.7 meq l^{-1} respectively. We observed very little change in SO_4^{2-} in the core taken 2 m from the seep site. However, H_2S, CH_4 and TA were enriched in the deeper sediment layers, relative to seawater,. Concentrations of all of these species in cores collected 5 and 10 m from the seep site were similar to seawater concentrations and varied little with depth.

Meiofaunal community structure

Meiofaunal densities were highest in the core taken 2 m from the seep site (3228.8 ind. 10 cm^{-2}). Although densities in the seep sediment core (794.8 ind. 10 cm^{-2}) and in the core taken at 5 m distance (825.3 ind. 10 cm^{-2}) were considerably lower, they were still elevated compared to those collected 10 (227.7 ind. 10 cm^{-2}), 100 (436.1 ind. 10 cm^{-2}) and 1100 m (424.3 ind. 10 cm^{-2}) from the seep site (Fig. 3). Nematodes were the most abundant (88.7 – 94.5 %) in all cores (Table 2). Meiofaunal densities in the seep sediment core below 1 cm, decreased sharply (Fig. 2). In comparison, densities in the core taken 2 m from the seep site decreased more gradually with depth. Meiofauna in the 2 cores retrieved farthest from seep influence penetrated deepest in the sediment.

Nematode size

Overall, total nematode biomass in the top 5 cm of the seep sediment core was almost 10x higher than that in the core taken 1100 m away (Fig. 3). Individual nematode size measurements (i.e. length, width, and biomass) differed significantly among cores ($p < 0.001$; Fig. 4) and peaked in the seep sediment core. Also nematode length/width ratios

varied significantly among cores ($p < 0.001$), with lowest ratios in the seep sediment core (Fig. 4C). *S. vasicola* and *S. punctata*, which dominated the seep sediment core, were on average 2416.5 ± 396.5 (n = 42) and 1130.8 ± 463.1 (n = 33) µm long respectively.

Nematode community structure

Nematode genus composition varied little among cores (Fig. 5, Table 3). *Sabatieria* dominated all samples, except at 2 m from the seep site, where *Rhabdocoma* (23 %) prevailed. All diversity indices correlated positively with distance from the seep site (Fig. 6), but these correlations were significant only for N_0 and EG(100) (N_0: $r = 0.93$, $p = 0.008$ and EG(100): $r = 0.81$, $p = 0.049$). *Desmodora* was only abundant (i.e. ≥1% of total) in cores within 5 m off the seep (Table 3).

Nematode feeding ecology

$\delta^{13}C$ ranged between -40.7 ‰ and -21.3 ‰, and $\delta^{15}N$ varied between 0.9 and 15.3 ‰ (Fig. 7). $\delta^{13}C$ ($r = 0.34$, $p = 0.14$) and $\delta^{15}N$ ($r = 0.24$, $p = 0.28$) became heavier with increasing distance from the seep site, though the correlations were not significant. No clear pattern emerged when plotting stable isotope signatures vs. sediment depth (Fig. 7). "Mix" ($\delta^{13}C$: -31.2 ± 4.9 ‰, $\delta^{15}N$: 7.11 ± 3.9 ‰) was significantly more enriched in ^{13}C ($p = 0.02$) and ^{15}N ($p = 0.02$) than *Desmodora* ($\delta^{13}C$: -38.5 ± 2.0 ‰, $\delta^{15}N$: 4.6 ± 2.2 ‰). *Sabatieria* ($\delta^{13}C$: -36.3 ± 2.4 ‰, $\delta^{15}N$: 6.9 ± 1.5 ‰) and *Desmodora* displayed similar isotope values ($\delta^{13}C$: $p = 0.67$, $\delta^{15}N$: $p = 0.43$). Based on buccal morphology, deposit-feeders (1A + 1B) dominated all cores (data not shown), although trophic diversity increased with increasing distance from the seep site ($r = 0.70$, $p = 0.12$), and leveled off at 10 m distance.

TEM and STEM-EDX

TEM revealed several, but mostly disintegrated bacteria bordering the cuticle of *Desmodora* (Fig. 9). Additionally, electron-lucent structures were observed near the cuticle (Fig. 9B). STEM-EDX analysis showed these contained trace amounts of sulphur. We observed no symbionts or detoxification structures in *Sabatieria*.

DISCUSSION

CH_4 seepage and spatial variability in pore-water geochemistry

Elevated pore-water CH_4 levels in the Darwin MV seep sediment core indicated a CH_4 flux from below the sediment surface, corroborating the gas escape from the seep sediments during sampling. However, CH_4 concentrations dropped from 1 mM down to <0.001 mM over a 10-m distance, suggesting focused flow. Pore-fluid analyses indicated some anaerobic consumption by microbes (i.e. anaerobic oxidation of methane or AOM): SO_4^{2} decreased rapidly with depth in the seep site pore-fluids, accompanied by an increase in TA and elevated H_2S concentrations (Reeburgh, 1976, Boetius et al. 2000, Knittel & Boetius 2009). The relatively small enrichments in H_2S, CH_4 and TA in the core taken 2 m from the seep site, suggest AOM presence here as well, but likely concentrated at depths exceeding the core length. The constancy in the concentrations of SO_4^{2}, TA, H_2S and CH_4 with depth in the cores taken at 5 and 10 m distance, suggest an absence of AOM. The high spatial variability in CH_4 flow at the Darwin MV illustrates the difficulty in taking replicate samples for pore-water geochemistry and associated fauna at seeps.

Impact of pore-water geochemistry on meiofaunal distribution and tolerance to high H_2S levels

At the Darwin MV, meiofaunal densities were much higher in and immediately near the seep site (2 m) compared to the sites showing no sign of seep influence in terms of pore-water geochemistry. Accordingly, Vanreusel et al. (2010) showed elevated meiofaunal

standing stock in seep compared to non-seep sediments for several other seep systems. The seep sediment core had high H_2S content (up to 22 mM), as shown for several other seeps (Barry et al. 1997, Levin et al. 2003, Sahling et al. 2002). These high H_2S levels impacted the vertical distribution in the sediment, in that the proportion of meiofauna confined to the sediment surface was highest in this core. Tolerance of high H_2S levels was genus (and species) specific. *Sabatieria* and *Desmodora*, which dominated the seep sediment core, were more tolerant to high H_2S than genera absent from this core.

In sulphidic environments, bacterial symbionts can help to detoxify H_2S (Ott et al. 2004). In bathyal oxygen minimum zone sediments, *Desmodora masira* had ectosymbionts (Bernhard et al. 2000). Although in our study, TEM cross-sections paralleled the annuli (in contrast to Bernhard et al. 2000), the low and irregular bacterial appearance implies that *Desmodora* from the seep sediment core did not harbour ectosymbionts. TEM showed electron-lucent structures near the cuticle resembling the sulphur inclusions described by Thiermann et al. (2000), but STEM-EDX analysis only detected traces of sulphur. However, elemental sulphur is known to leach from vesicles during chemical fixation, dehydration, and resin infiltration of biological samples, which may explain the low sulphur content (Lechaire et al. 2006). Increased body length is another adaptation to sulphidic conditions, and enables a fast migration between anoxic, sulphidic, and oxic, H_2S-free sediments (Schratzberger et al. 2004, Levin 2005). Accordingly, *S. punctata*, and *S. vasicola*, which dominated the seep sediment core, were amongst the longest nematodes in this study.

Meiofaunal and nematode community structure

Meiofaunal density patterns were mainly driven by the dominant taxon, i.e. the nematodes. Nematodes dominate most seep habitats (Shirayama & Ohta 1990, Robinson et al. 2004, Van

272 Gaever et al. 2009a, Van Gaever et al. 2009c), although some habitats are dominated by
273 copepods (Van Gaever et al. 2006). In the Darwin MV seep sediment core, meiofauna-sized
274 polychaetes were subdominant, similar to the REGAB mussel beds (Van Gaever et al. 2009a).

275 Nematode genus composition clearly differed between cores with and without CH_4
276 flow. Thus, CH_4 flow affected not only densities and biomass, but also composition. Genus
277 diversity was lowest in the seep sediment core and increased in cores farther from the seep
278 site, as shown in previous studies (Van Gaever et al. 2009a,c). *Desmodora* and *Sabatieria*
279 also dominated the REGAB seep in the Gulf of Guinea (Van Gaever et al. 2009a), although in
280 association with different habitats: the REGAB samples originated from clam and mussel
281 fields with low H_2S content (<0.1 µM; Olu-Le Roy et al. 2009). *S. vasicola* and *S. punctata*,
282 which dominated the Darwin MV seep sediment core, also occur in shallow waters (Vitiello
283 1970, Jensen et al. 1992, Franco et al. 2008). Accordingly, the dominant species at the
284 REGAB seep (*S. mortenseni*), the Arctic Håkon Mosby MV (*Halomonhystera disjuncta)* (Van
285 Gaever et al. 2006), and the Nordic Nyegga seep (*Terschellingia longicaudata*) (Van Gaever
286 et al. 2009c) inhabit shallow waters as well. The presence of these species in both shallow
287 waters and at a deep-sea seep suggests a possible connection between these habitats,
288 rather than between deep-sea seeps (Van Gaever et al. 2009c).

289 **Feeding ecology**

290 $\delta^{13}C$ values suggest thiotrophic C is part of the nematode diet up to 10 m from the seep site.
291 Except for "Mix" in sediment layer 4-6 cm, which displays a $\delta^{13}C$ of -21.3 ‰, all $\delta^{13}C$ were
292 less than -28 ‰. Organic matter produced through sulphur-oxidation has an average $\delta^{13}C$ of
293 -30 ‰ (RubisCO I) or -11 ‰ (RubisCO II), depending on the Rubisco enzyme involved
294 (Robinson & Cavanaugh 1995). In comparison, photosynthetic C is characterized by $\delta^{13}C$

between -18 and -28 ‰ (Stewart et al. 2005), and CH_4-derived C is more depleted in ^{13}C ($\delta^{13}C$ < -50 ‰) (Levin & Michener 2002). Since we did not sample potential C sources for stable isotope analysis, we cannot estimate their relative contribution to the nematode diet. Nonetheless, a decrease in thiotrophic (RubisCO I) and an increase in photosynthetic C in the nematode diet farther from the seep site are implied by (1) the thicker hemipelagic sediment veneer on top of the cores, suggesting a higher availability of photosynthetic C, (2) an increase in trophic diversity, and (3) heavier $\delta^{13}C$.

Spies et al. (1983) and Van Gaever et al. (2006, 2009b) reported direct nematode consumption of sulphur-oxidisers. These bacteria live at the interface between oxic and anoxic sediments, where H_2S levels are ≤1 µM (Robertson & Kuenen 2006, Preisler et al. 2007). We doubt these bacteria inhabited the seep sediments given the absence of bacterial mats and the high H_2S levels at greater depth. In the core collected 2 m from the seep site, we observed no net SO_4^{2-} production, expected in the presence of sulphur-oxidisers. Nematodes can indirectly consume sulphur-oxidisers by assimilating dissolved organic matter (DOM) released upon bacterial lysis. Jensen (1987) suggested thiobiotic nematodes feed, at least partially, on DOM. However, further evidence is needed to support this hypothesis. Stable isotope signatures suggest different feeding strategies for *Sabatieria* and *Desmodora* compared with the bulk nematode community, which may explain their success. As with other seeps (Vanreusel et al. 2010), deposit-feeders dominated. Finally, although this exploratory study hints at how meiofauna interacts with the seep environment, much more, high-resolution research is required to understand their tolerance of sulphide, trophic interactions, and dispersal capacities.

Acknowledgements. The research leading to these results has received funding from the European Community's Seventh Framework Programme (FP7/2007-2013) under the HERMIONE project, grant agreement n° 226354 and was supported by the FWO “cold seeps” project n° G034607. The authors are greatly indebted to the crew and the captain of the *RRS* James Cook and the pilots of ROV Isis for their expertise and

professionalism. We also gratefully acknowledge M. Claeys for her assistance and the preparation of the TEM photographs. Finally yet importantly, we greatly appreciated the comments of the editor, the reviewers, and Lois Maignien.

LITERATURE CITED

Andrassy I (1956) The determination of volume and weight of nematodes. Acta Zool Hung 2:1-15

Barry JP, Kochevar RE, Baxter CH (1997) The influence of pore-water chemistry and physiology on the distribution of vesicomyid clams at cold seeps in Monterey Bay: implications for patterns of chemosynthetic community organization. Limnol Oceanogr 42:318-328

Bernhard JM, Buck KR, Farmer MA, Bowser SS (2000) The Santa Barbara Basin is a symbiosis oasis. Nature 403:77-80

Boetius A, Ravenschlag K, Schubert CJ, Rickert D, Widdel F, Gieseke A, Amann R, Jorgensen BB, Witte U, Pfannkuche O (2000) A marine microbial consortium apparently mediating anaerobic oxidation of methane. Nature 407:623-626

Carman KR, Fry B (2002) Small-sample methods for delta $\delta^{13}C$ and delta $\delta^{15}N$ analysis of the diets of marsh meiofaunal species using natural-abundance and tracer-addition isotope techniques. Mar Ecol Prog Ser 240:85-92

Clarke K, Gorley R (2006) PRIMER v6: User Manual/tutorial. Primer-E Ltd, Plymouth

Dando PR, Austen MC, Burke RA, Kendall MA, Kennicutt MC, Judd AG, Moore DC, O'Hara SCM, Schmaljohann R, Southward AJ (1991) Ecology of a North Sea pockmark with an active methane seep. Mar Ecol Prog Ser 70:49-63

Franco MA, Soetaert K, Van Oevelen D, Van Gansbeke D, Costa MJ, Vincx M, Vanaverbeke J (2008) Density, vertical distribution and trophic responses of metazoan meiobenthos to phytoplankton deposition in contrasting sediment types. Mar Ecol Prog Ser 358:51-62

Genio L, Johnson SB, Vrijenhoek RC, Cunha MR, Tyler PA, Kiel S, Little CTS (2008) New record of "Bathymodiolus" mauritanicus Cosel 2002 from the Gulf of Cadiz (NE Atlantic) mud volcanoes. J Shellfish Res 27:53-61

Grasshoff K, Ehrhardt M, Kremling K, Anderson L (1999) Methods of seawater analysis. Wiley-VCH, Weinheim

Heip C, Vincx M, Vranken G (1985) The ecology of marine nematodes. Oceanogr Mar Biol Annu Rev 23:399-489

Helms J, Munzel U (2008) npmc: Nonparametric Multiple Comparisons. R package version 10-7

Hoehler T, Borowski W, Alperin M, Rodriguez N, Paull C (2000) Model, stable isotope and radiotracer characterization of anaerobic methane oxidation in gas hydrate-bearing sediments of the blake ridge. Proc Ocean Drilling Prog: Sci Results 164:79-85

Ivanenkov V, Lyakhin Y (1978) Determination of total alkalinity in seawater. In: Methods of hydrochemical investigations in the ocean. Nauka Publ. House, Moscow, p 110–114

Jensen P (1984) Measuring carbon content in nematodes. Helgolander Meeresun 38:83-86

Jensen P (1987) Feeding ecology of free-living aquatic nematodes. Mar Ecol Prog Ser 35:187-196

Jensen P, Aagaard I, Burke RA, Dando PR, Jorgensen NO, Kuijpers A, Laier T, Ohara SCM, Schmaljohann R (1992) 'Bubbling Reefs' in the Kattegat: submarine landscapes of carbonate-cemented rocks support a diverse ecosystem at methane seeps. Mar Ecol Prog Ser 83:103-112

Knittel K, Boetius A (2009) Anaerobic oxidation of methane: progress with an unknown process. Annu Rev Microbiol 63:311-334

Lambshead PJD, Boucher G (2003) Marine nematode deep-sea biodiversity - hyperdiverse or hype? J Biogeogr 30:475-485

Lechaire JP, Frebourg G, Gaill F, Gros O (2006) In situ localization of sulphur in the thioautotrophic symbiotic model Lucina pectinata (Gmelin, 1791) by cryo-EFTEM microanalysis. Biol Cell 98:163-170

370 Levin LA, Michener RH (2002) Isotopic evidence for chemosynthesis-based nutrition of
371 macrobenthos: The lightness of being at Pacific methane seeps. Limnol Oceanogr 47:1336-
372 1345
373 Levin LA, Ziebis W, Mendoza GF, Growney VA, Tryon MD, Brown KM, Mahn C, Gieskes JM, Rathburn
374 AE (2003) Spatial heterogeneity of macrofauna at northern California methane seeps:
375 influence of sulfide concentration and fluid flow. Mar Ecol Prog Ser 265:123-139
376 Levin LA (2005) Ecology of cold seep sediments: Interactions of fauna with flow, chemistry and
377 microbes. Oceanogr Mar Biol Annu Rev 43:1-46
378 Middelburg JJ, Soetaert K, Herman PMJ (1997) Empirical relationships for use in global diagenetic
379 models. Deep-Sea Res I 44:327-344
380 Munzel U, Hothorn LA (2001) A unified approach to simultaneous rank test procedures in the
381 unbalanced one-way layout. Biom J 43:553-569
382 Olu-Le Roy K, Lance S, Sibuet M, Henry P, FialaMedioni A, Dinet A (1997) Cold seep communities as
383 indicators of fluid expulsion patterns through mud volcanoes seaward of the Barbados
384 accretionary prism. Deep-Sea Res I 44:811-841
385 Olu-Le Roy K, Caprais JC, Galéron J, Causse R, von Cosel R, Budzinski H, Ménach KL, Roux CL, Levaché
386 D, Khripounoff A (2009) Influence of seep emission on the non-symbiont-bearing fauna and
387 vagrant species at an active giant pockmark in the Gulf of Guinea (Congo–Angola margin).
388 Deep-Sea Res II 56:2380-2393
389 Ott J, Bright M, Bulgheresi S (2004) Symbioses between marine nematodes and sulfur-oxidizing
390 chemoautotrophic bacteria. Symbiosis 36:103-126
391 Pinheiro LM, Ivanov MK, Sautkin A, Akhmanov G, Magalhaes VH, Volkonskaya A, Monteiro JH,
392 Somoza L, Gardner J, Hamouni N (2003) Mud volcanism in the Gulf of Cadiz: results from the
393 TTR-10 cruise. Mar Geol 195:131-151
394 Post DM (2002) Using stable isotopes to estimate trophic position: Models, methods, and
395 assumptions. Ecology 83:703-718
396 Preisler A, de Beer D, Lichtschlag A, Lavik G, Boetius A, Jorgensen BB (2007) Biological and chemical
397 sulfide oxidation in a Beggiatoa inhabited marine sediment. Isme J 1:341-353
398 Qi HP, Coplen TB, Geilmann H, Brand WA, Bohlke JK (2003) Two new organic reference materials $\delta^{13}C$
399 and $\delta^{15}N$ measurements and a new value for the $\delta^{13}C$ of NBS 22 oil. Rapid Commun Mass
400 Spectrom 17:2483-2487
401 R Development Core Team (2010) R: A language and environment for statistical computing. R
402 Foundation for Statistical Computing, Vienna, available at http://www.R-project.org
403 Reeburgh WS (1976) Methane consumption in Cariaco Trench waters and sediments. Earth Planet Sc
404 Lett 28:337-344
405 Reeburgh WS (2007) Oceanic methane biogeochemistry. Chem Rev 107:486-513
406 Robertson L, Kuenen J (2006) The Colorless Sulfur Bacteria. In: Dworkin M, Falkow S, Rosenberg E,
407 Schleifer K-H, Stackebrandt E (eds) The Prokaryotes: ecophysiology and biochemistry.
408 Springer, New York, p 985-1011
409 Robinson C, Bernhard J, Levin L, Mendoza G, Blanks J (2004) Surficial hydrocarbon seep infauna from
410 the Blake Ridge(Atlantic Ocean, 2150 m) and the Gulf of Mexico(690-2240 m). Mar Ecol
411 25:313-336
412 Robinson JL, Cavanaugh CM (1995) Rubisco in chemoautotrophic symbioses: Implications for the
413 interpretation of stable carbon isotope values. Limnol Oceanogr 40:1496-1502
414 Sahling H, Rickert D, Lee RW, Linke P, Suess E (2002) Macrofaunal community structure and sulfide
415 flux at gas hydrate deposits from the Cascadia convergent margin, NE Pacific. Mar Ecol Prog
416 Ser 231:121-138
417 Schratzberger M, Whomersley P, Warr K, Bolam SG, Rees HL (2004) Colonisation of various types of
418 sediment by estuarine nematodes via lateral infaunal migration: a laboratory study. Mar Biol
419 145:69-78
420 Seeberg-Elverfeldt J, Schlüter M, Feseker T, Kölling M (2005) Rhizon sampling of pore waters near the
421 sediment/water interface of aquatic systems. Limnol Oceanogr- Meth 3:361-371

Shirayama Y, Ohta S (1990) Meiofauna in a cold-seep community off Hatsushima, Central Japan. J Oceanogr 46:118-124
Soetaert K, Franco M, Lampadariou N, Muthumbi A, Steyaert M, Vandepitte L, vanden Berghe E, Vanaverbeke J (2009) Factors affecting nematode biomass, length and width from the shelf to the deep sea. Mar Ecol Prog Ser 392:123-132
Somoza L, Diaz-del-Rio V, Leon R, Ivanov M, Fernandez-Puga MC, Gardner JM, Hernandez-Molina FJ, Pinheiro LM, Rodero J, Lobato A, Maestro A, Vazquez JT, Medialdea T, Fernandez-Salas LM (2003) Seabed morphology and hydrocarbon seepage in the Gulf of Cadiz mud volcano area: acoustic imagery, multibeam and ultra-high resolution seismic data. Mar Geol 195:153-176
Spies R, DesMarais D (1983) Natural isotope study of trophic enrichment of marine benthic communities by petroleum seepage. Mar Biol 73:67-71
Stewart FJ, Newton ILG, Cavanaugh CM (2005) Chemosynthetic endosymbioses: adaptations to oxic-anoxic interfaces. Trends Microbiol 13:439-448
Thierman F, Vismann B, Giere O (2000) Sulphide tolerance of the marine nematode Oncholaimus campylocercoides – a result of internal sulphur formation? Mar Ecol Prog Ser 193: 251-259
Thurber AR, Kröger K, Neira C, Wiklund H, Levin LA (2009) Stable isotope signatures and methane use by New Zealand cold seep benthos. Mar Geol 272:260-269
Van Gaever S, Moodley L, de Beer D, Vanreusel A (2006) Meiobenthos at the Arctic Hakon Mosby Mud Volcano, with a parental-caring nematode thriving in sulphide-rich sediments. Mar Ecol Prog Ser 321:143-155
Van Gaever S, Galéron J, Sibuet M, Vanreusel A (2009a) Deep-sea habitat heterogeneity influence on meiofaunal communities in the Gulf of Guinea. Deep-Sea Res II 56:2259-2269
Van Gaever S, Moodley L, Pasotti F, Houtekamer M, Middelburg JJ, Danovaro R, Vanreusel A (2009b) Trophic specialisation of metazoan meiofauna at the Hakon Mosby Mud Volcano: fatty acid biomarker isotope evidence. Mar Biol 156:1289-1296
Van Gaever S, Olu-Le Roy K, Derycke S, Vanreusel A (2009c) Metazoan meiofaunal communities at cold seeps along the Norwegian margin: influence of habitat heterogeneity and evidence for connection with shallow-water habitats. Deep-Sea Res I 56:772-785
Van Rensbergen P, Depreiter D, Pannemans B, Moerkerke G, Van Rooij D, Marsset B, Akhmanov G, Blinova V, Ivanov M, Rachidi M, Magalhaes V, Pinheiro L, Cunha M, Henriet J-P (2005) The El Arraiche mud volcano field at the Moroccan Atlantic slope, Gulf of Cadiz. Mar Geol 219:1-17
Vanreusel A, Andersen AC, Boetius A, Connelly D, Cunha MR, Decker C, Hilario A, Kormas KA, Maignien L, Olu K, Pachiadaki M, Ritt B, Rodrigues CF, Sarrazin J, Tyler PA, Van Gaever S, Vanneste H (2009) Biodiversity of cold seep ecosystems along the European margins. Oceanography 22:110-127
Vanreusel A, De Groote A, Gollner S, Bright M (2010) Ecology and biogeography of free-living nematodes associated with chemosynthetic environments in the deep sea: a review. Plos One 5:1-15
Vitiello P (1970) Nématodes libres marins des vases profondes du Golfe du Lion. II Chromadorida. Téthys 2:449-500
Wieser W (1952) Die Beziehung zwischen Mundhöhlengestalt, Ernährungsweise und Vorkommen bei freilebenden marinen Nematoden. Eine ökologisch-morphologische Studie. Arkiv för Zoologi 4:439-483

FIGURE CAPTIONS

Fig. 1. (A) Bathymetric map of the Darwin MV with the core locations on the MV indicated (©NOC 2009) (B) Schematic representation of the sampling strategy. PUC1: push core 1,

469 sampled for pore-water geochemistry and meiofaunal community analyses; PUC2: push core
470 2, sampled for pore-water CH_4 concentration, porosity and nematode stable isotope
471 signatures; MC: megacorer, sampled for meiofaunal community analyses

472 Fig. 2. Vertical pore-water profiles of H_2S, SO_4^{2-}, CH_4 and TA, and sedimentary densities of
473 nematodes and other meiofaunal taxa in relation to distance from the Darwin MV seep site.
474 Vertical arrows indicate seawater values. Note the different scales on the graphs

475 Fig. 3. Total nematode densities and biomass in relation to distance from the Darwin MV
476 seep site (0-5 cm)

477 Fig. 4. Mean nematode (A) length, (B) width, (C) length/width and (D) biomass in function of
478 sediment depth (cm), in relation to distance from the Darwin MV seep site

479 Fig.5. MDS plot of standardized genera-abundance data in relation to distance from the
480 Darwin MV seep site. Numbers indicate sediment depth (cm). Contour plots were not drawn
481 for the cores collected at 100 and 1100 m from the seep site as these overlapped

482 Fig. 6. Ln-transformed diversity indices based on nematode genera abundances in relation to
483 distance from the Darwin MV seep site. N_0, N_1, N_{inf}: Hill's numbers; J': Pielou's evenness
484 number; H': Shannon-Wiener Diversity index; EG(100): expected number of genera for
485 n=100

486 Fig. 7. *Desmodora* (Des), *Sabatieria* (Sab) and "Mix" (A) C and (B) N isotope signatures in
487 relation to distance from the Darwin MV seep site. At 10-m distance, no $\delta^{13}C$ was available
488 for 0-2 cm due to the low amount of C, making the isotope value unreliable. Colours
489 represent sediment layers (white: 0-2 cm, grey: 2-4 cm, black: 4-6 cm)

490 Fig. 8. Nematode trophic diversity in relation to distance from the Darwin MV seep site (0-5
491 cm)

492 Fig. 9. TEM micrograph of a cross-section of *Desmodora* from the Darwin MV seep sediment
493 core. (A) Overview, (B) Detail showing bacteria associated with the cuticle. The white arrow
494 points to empty structures, possibly containing S prior to ethanol dehydration. Ba: bacterial
495 cell

496

497 **FIGURES**

498 Fig. 1

499

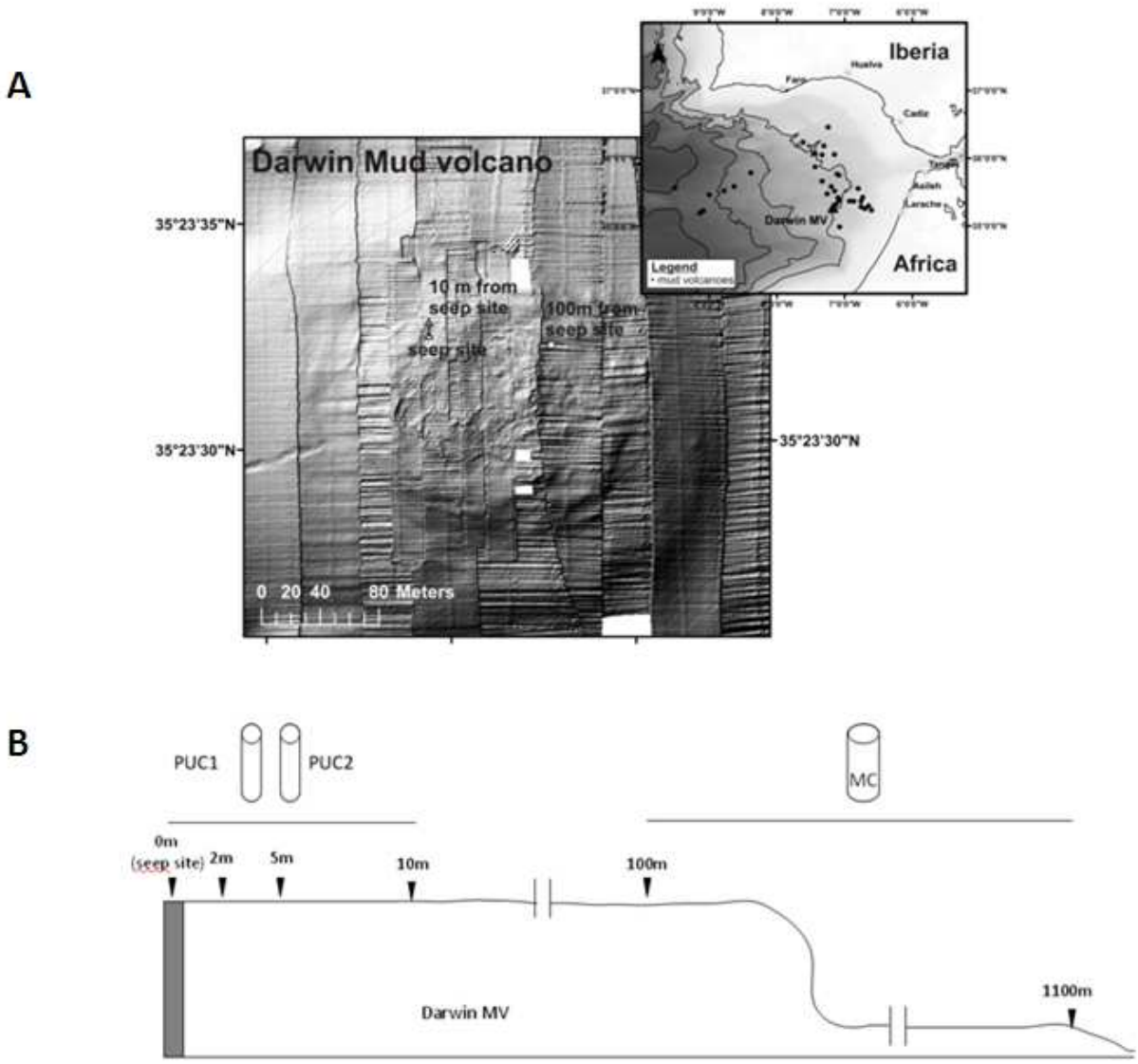

500

501

502

503 Fig. 2

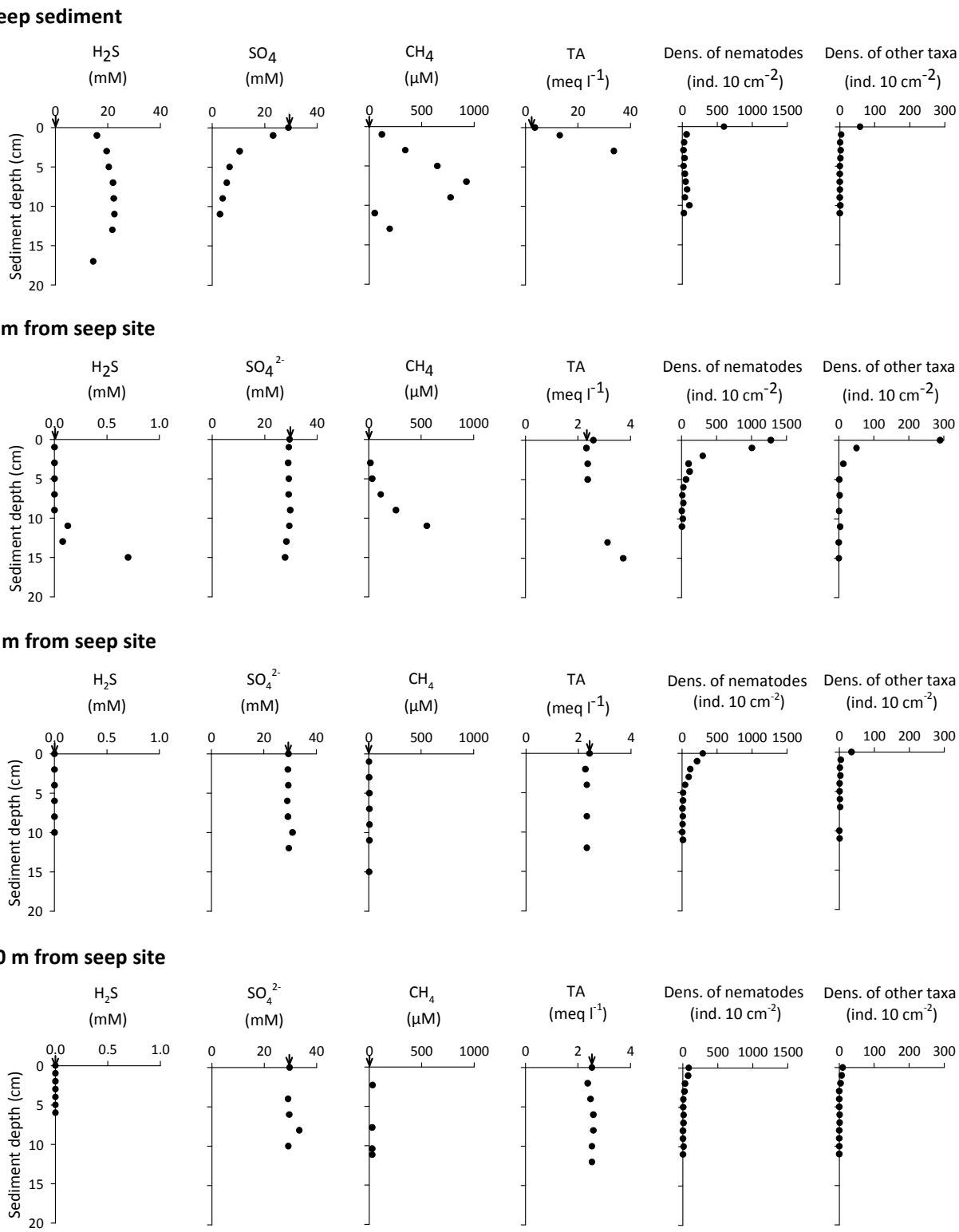
Seep sediment
2 m from seep site
5 m from seep site
10 m from seep site
H2S (mM)
SO4 (mM)
SO4 2- (mM)
CH4 (µM)
TA (meq l-1)
Dens. of nematodes (ind. 10 cm-2)
Dens. of other taxa (ind. 10 cm-2)
Sediment depth (cm)

Fig. 3

507

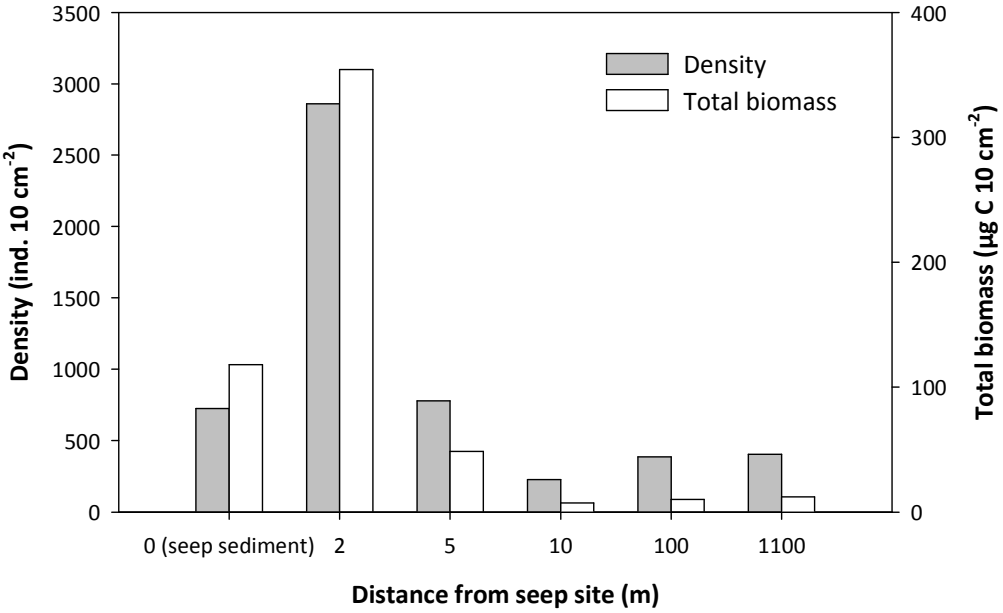
Density
Total biomass
Density (ind. 10 cm-2)
Total biomass (µg C 10 cm-2)
3500
3000
2500
2000
1500
1000
500
0
400
300
200
100
0
0 (seep sediment)
2
5
10
100
1100
Distance from seep site (m)

508

509 Fig. 4

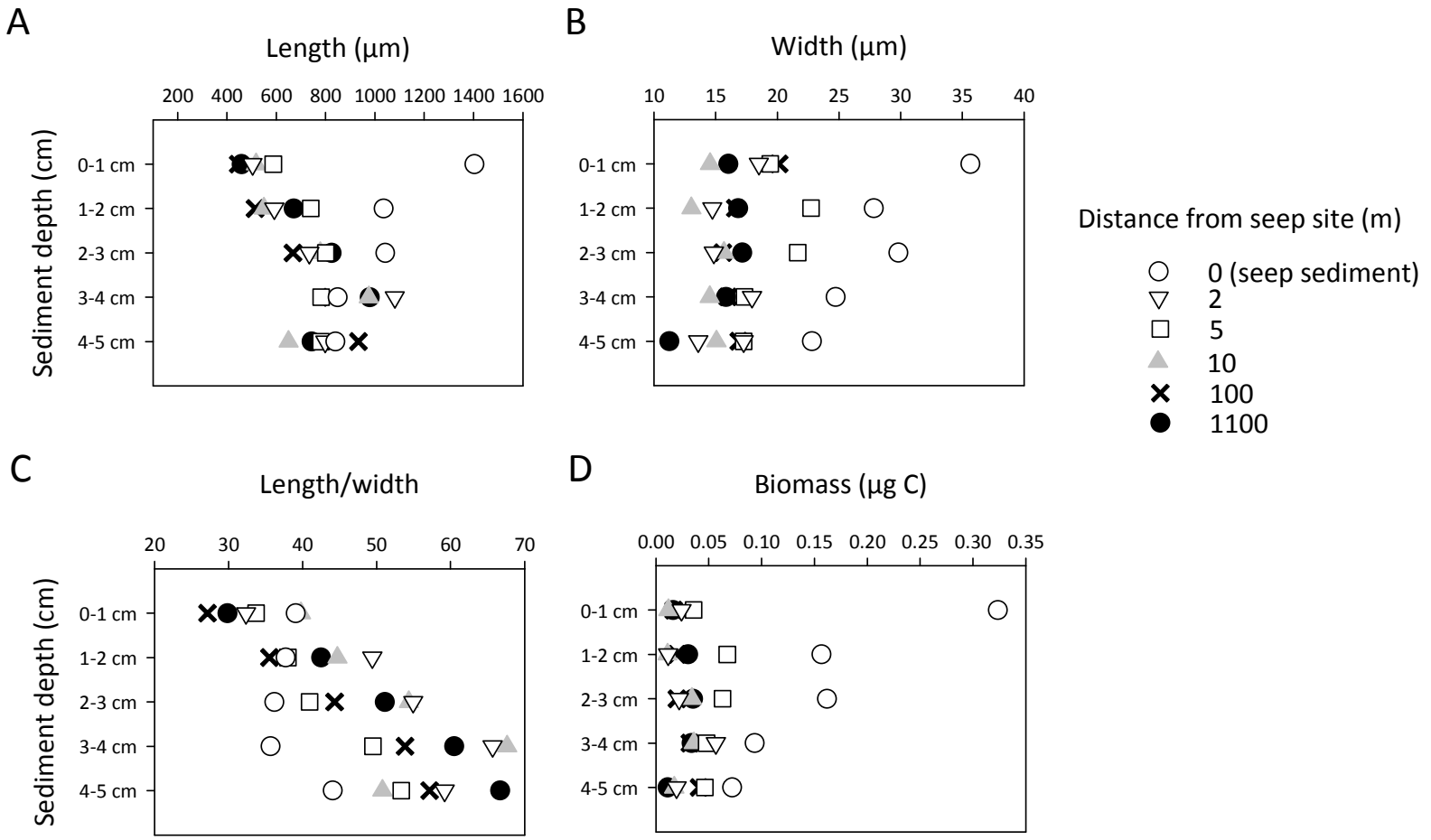
A
Length (µm)
200 400 600 800 1000 1200 1400 1600
Sediment depth (cm)
0-1 cm
1-2 cm
2-3 cm
3-4 cm
4-5 cm
B
Width (µm)
10 15 20 25 30 35 40
C
Length/width
20 30 40 50 60 70
D
Biomass (µg C)
0.00 0.05 0.10 0.15 0.20 0.25 0.30 0.35
Distance from seep site (m)
0 (seep sediment)
2
5
10
100
1100

510

511 Fig. 5

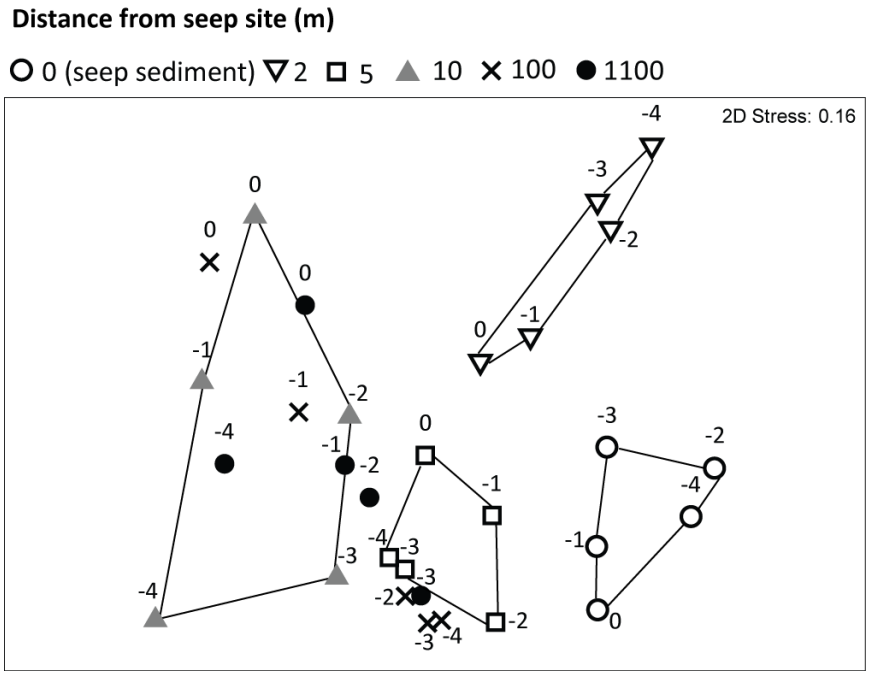

512

513 Fig. 6

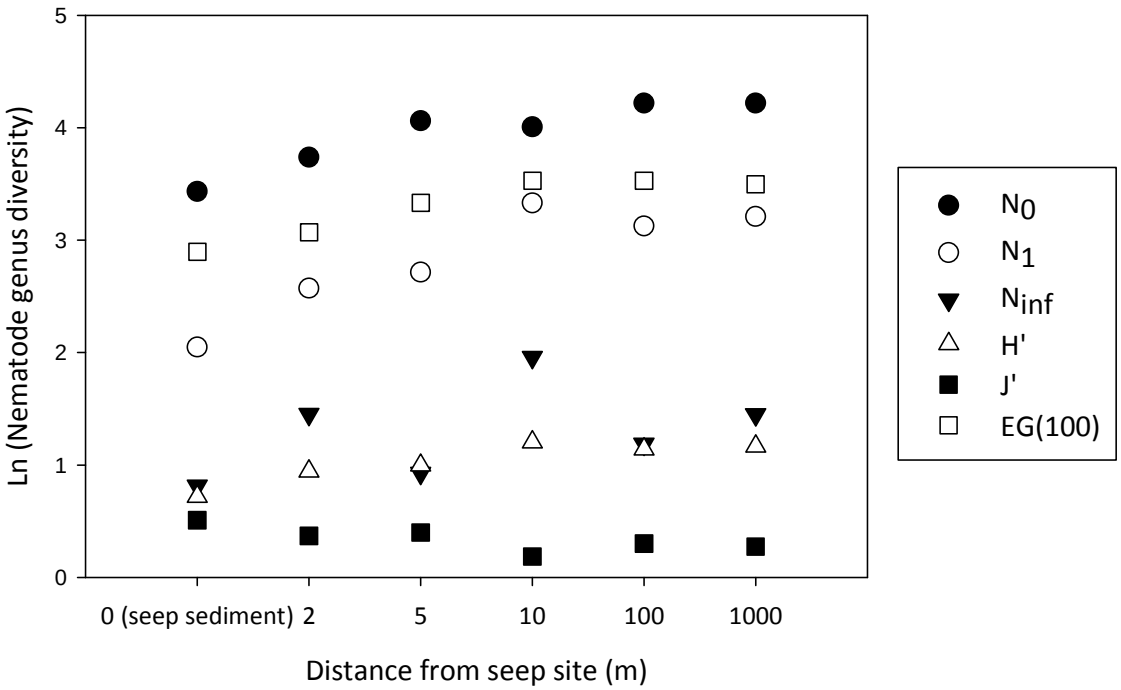

514

515

516

517 Fig. 7

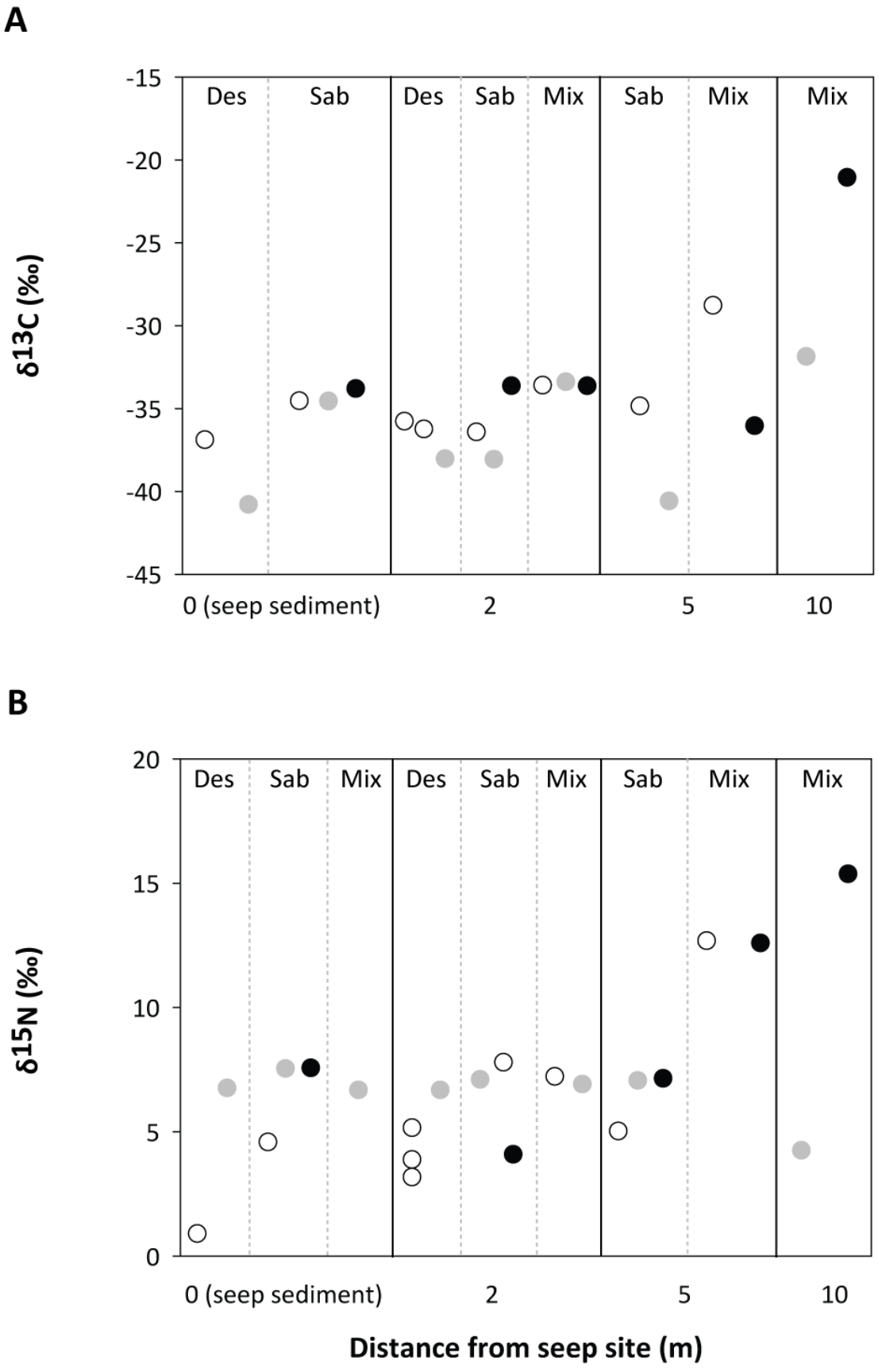
A
-15
-20
-25
-30
-35
-40
-45
δ13C (‰)
Des
Sab
Des
Sab
Mix
Sab
Mix
Mix
0 (seep sediment)
2
5
10
B
20
15
10
5
0
δ15N (‰)
Des
Sab
Mix
Des
Sab
Mix
Sab
Mix
Mix
0 (seep sediment)
2
5
10
Distance from seep site (m)

518

519 Fig. 8

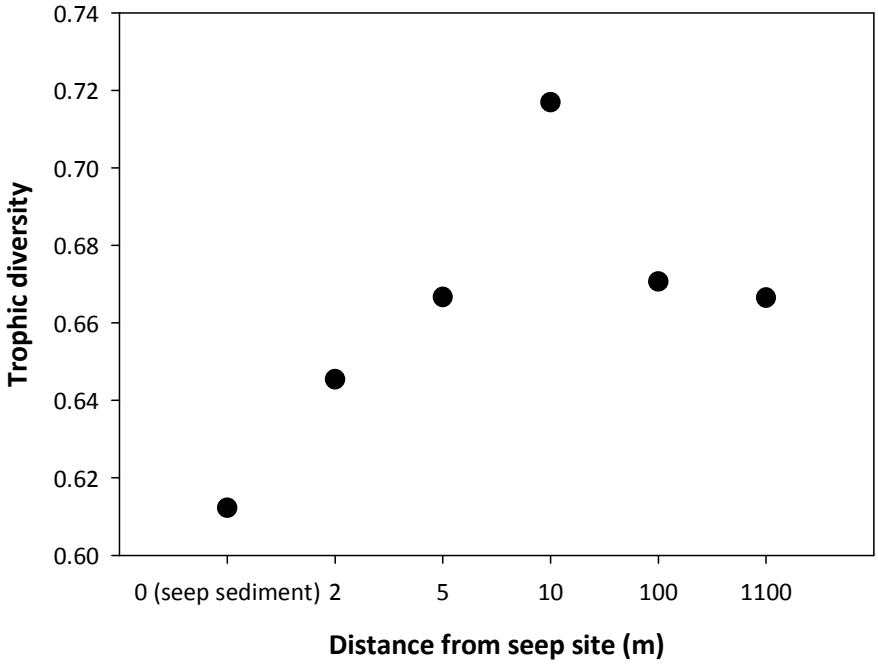

520

521 Fig. 9

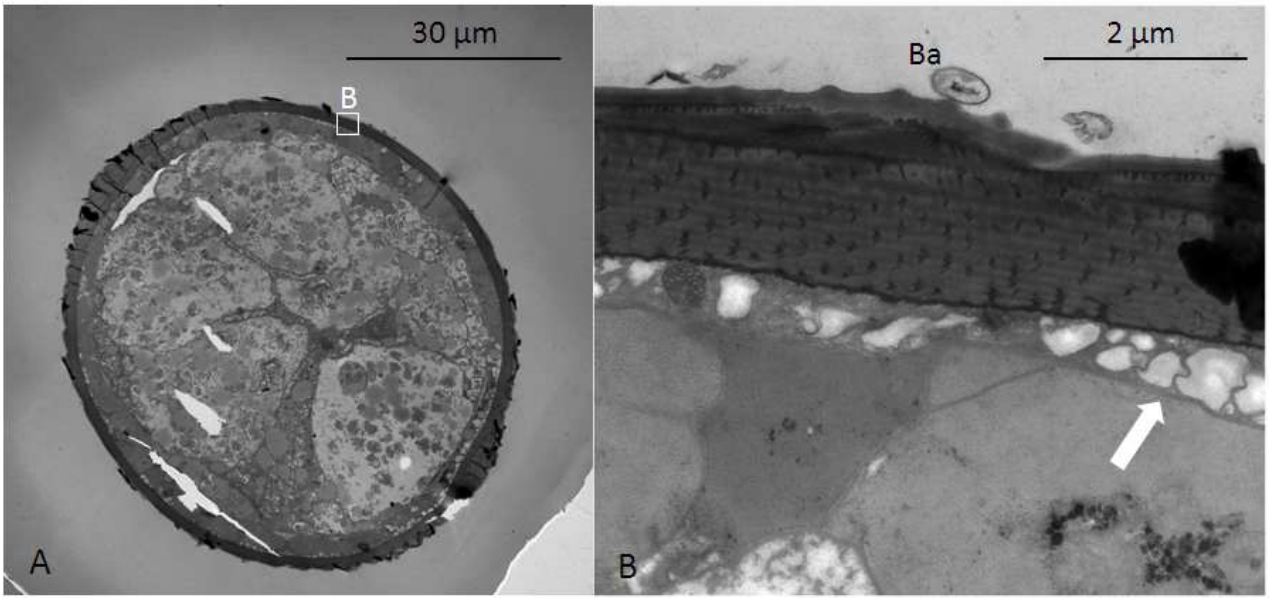

522

523 **TABLE CAPTIONS**

524 Table 1. Parameters of the sediment core locations in relation to distance from the Darwin MV
525 seep site. PUC: push core, MC: megacore

526 Table 2. Meiofaunal densities in relation to distance from the Darwin MV seep site (0-5 cm)

527 Table 3. Relative abundances of the most abundant nematode genera (≥1%) in relation to
528 distance from the Darwin MV seep site (0-5 cm)

529 Table 4. Relative abundances of *Sabatieria* species in relation to distance from the Darwin MV
530 seep site (0-5 cm)

531 **TABLES**

532 Table 1

Distance from seep site (m)	Position	Height hemipelagic layer (% core length)	Gear	N° of cores	Analyses
0 (seep sediment)	35°23.539'N, 7°11.508'W	0	PUC	2	PUC1: meiofaunal community structure and pore-water geochemistry PUC2: porosity, pore-water CH_4 concentration and nematode stable isotopes
2	35°23.543'N, 7°11.506'W	22-33	PUC	2	PUC1: meiofaunal community structure and pore-water geochemistry PUC2: porosity, pore-water CH_4 concentration and nematode stable isotopes
5	35°23.543'N, 7°11.509'W	53-63	PUC	2	PUC1: meiofaunal community structure and pore-water geochemistry PUC2: porosity, pore-water CH_4 concentration and nematode stable isotopes
10	35°23.547'N, 7°11.511'W	71	PUC	2	PUC1: meiofaunal community structure and pore-water geochemistry PUC2: porosity, pore-water CH_4 concentration and nematode stable isotopes
100	35°23.537'N, 7°11.454'W	100	MC	1	meiofaunal community structure
1100	35°23.965'N, 7°11.121'W	100	MC	1	meiofaunal community structure

533 Table 2

	Distance from seep site (m)					
Taxon	0 (seep sediment)	2	5	10	100	1100
Density (ind. 10 cm^{-2})						
Amphipoda		0.8				
Bivalvia	2.0		1.2		0.1	
Cladocera				0.4		
Cnidaria		4.3		0.8		0.3
Copepoda	7.84	121.9	12.5	3.9	16.9	7.7
Cumacea				0.4	0.3	0.1
Gastrotricha	0.4		1.6			
Halacaroidea	4.7	2.7	0.4			
Holothuroidea		1.2			7.7	0.4
Hydrozoa	0.4					
Isopoda		3.9	0.4	0.4	0.9	0.1
Kinorhyncha	0.8			0.4		
Nauplii	9.8	154.8	9.4	4.7	11.1	2.5
Nematoda	725.0	2860.1	779.5	227.7	387.9	405.4
Oligochaeta	0.8	9.8	5.1			0.1
Ostracoda		0.8	1.6		1.1	0.4
Polychaeta	42.7	54.5	7.1	9.8	8.7	5.9
Tanaidacea		3.5	0.8	0.4		
Tardigrada		8.6	5.9		1.5	1.2
Total	**794.4**	**3226.9**	**825.3**	**248.4**	**436.1**	**424.3**

534

535

536 Table 3

537

Distance from seep site (m)											
0 (seep sediment)		2		5		10		100		1100	
Sabatieria	44.2	*Rhabdocoma*	23.5	*Sabatieria*	39.3	*Sabatieria*	14.1	*Sabatieria*	30.3	*Sabatieria*	23.6
Desmodora	19.2	*Amphimonhystrella*	18.6	*Thalassomonhystera*	7.8	*Molgolaimus*	11.4	*Thalassomonhystera*	8.6	*Thalassomonhystera*	9.6
Ethmolaimidae n.gen.	8.2	*Sabatieria*	14.4	*Desmodora*	5.6	*Daptonema*	6.4	*Hopperia*	6.0	*Acantholaimus*	7.0
Desmoscolex	6.0	*Ethmolaimidae n.gen.*	8.0	*Acantholaimus*	4.4	*Acantholaimus*	6.0	*Acantholaimus*	5.0	*Amphimonhystrella*	5.7
Tricoma	2.5	*Daptonema*	6.3	*Molgolaimus*	4.0	*Thalassomonhystera*	5.7	*Molgolaimus*	3.4	*Theristus*	5.7
Amphimonhystrella	2.5	*Desmodora*	5.3	*Microlaimus*	3.8	*Halalaimus*	4.4	*Diplopeltula*	2.8	*Halalaimus*	4.1
Linhomeus	2.2	*Tricoma*	3.8	*Halalaimus*	3.8	*Theristus*	4.4	*Halalaimus*	2.6	*Hopperia*	4.1
Comesa	1.6	*Linhomeus*	1.9	*Aegialoalaimus*	2.0	*Amphimonhystrella*	4.0	*Leptolaimus*	2.4	*Molgolaimus*	2.7
Thalassomonhystera	1.1	*Molgolaimus*	1.7	*Hopperia*	2.0	*Syringolaimus*	3.4	*Amphimonhystrella*	2.2	*Leptolaimus*	2.5
Cyartonema	1.1	*Thalassomonhystera*	1.5	*Amphimonhystrella*	2.0	*Sphaerolaimus*	3.0	*Greefiella*	1.7	*Diplopeltula*	2.3
		Theristus	1.5	*Syringolaimus*	1.8	*Nemanema*	2.7	*Microlaimus*	1.7	*Aegialoalaimus*	2.1
		Microlaimus	1.3	*Desmoscolex*	1.6	*Leptolaimus*	2.4	*Theristus*	1.7	*Syringolaimus*	2.1
		Leptolaimoides	1.1	*Tricoma*	1.5	*Microlaimus*	2.4	*Desmoscolex*	1.5	*Cervonema*	1.8
				Monhystrella	1.1	*Halichoanolaimus*	2.4	*Halichoanolaimus*	1.5	*Daptonema*	1.8
				Leptolaimus	1.1	*Aegialoalaimus*	2.4	*Cervonema*	1.4	*Neochromadora*	1.8
				Nyctonema	1.1	*Oxystomina*	1.7	*Neochromadora*	1.4	*Doliolaimus*	1.4
				Rhabdocoma	1.1	*Neochromadora*	1.7	*Aegialoalaimus*	1.2	*Oxystomina*	1.4
						Rhabdocoma	1.7	*Monhystrella*	1.2	*Desmoscolex*	1.2
						Linhystera	1.3	*Oxystomina*	1.2	*Leptolaimoides*	1.2
						Leptolaimoides	1.3	*Campylaimus*	1.0	*Microlaimus*	1.2
						Hopperia	1.3	*Linhystera*	1.0		
						Prototricoma	1.0	*Omicronema*	1.0		
						Metadesmolaimus	1.0	*Paracomesoma*	1.0		
						Linhomeus	1.0	*Prototricoma*	1.0		
								Syringolaimus	1.0		

538

539

Table 4

Distance from seep site (m)											
0 (seep sediment)		2		5		10		100		1100	
Species	%	Species	%	Species	%	Species	%	Species	%	Species	%
S. vasicola	28.5	*S. bitumen*	38.0	*S. bitumen*	40.7	*S. bitumen*	39.5	*S. ornata*	10.5	*S. stekhoveni*	51.6
S. punctata	20.8	*S. ornata*	34.7	*S. aff. breviseta*	16.3	*S. stekhoveni*	19.7	*S. bitumen*	10.2	*S. aff. breviseta*	9.5
S. stekhoveni	18.2	*S. propisinna*	17.5	*S. propisinna*	16.3	*S. ornata*	15.8	*S. demani*	7.2	*S. propisinna*	7.9
S. ornata	10.1	*S. stekhoveni*	9.7	*S. demani*	12.2	*S. propisinna*	13.2	*S. stekhoveni*	5.2	*S. conicauda*	6.7
S. aff. breviseta	8.3			*S. stekhoveni*	11.7	*S. demani*	11.8	*S. aff. breviseta*	3.4	*S. demani*	5.7
S. conicauda	4.7			*S. ornata*	2.7			*S. conicauda*	2.7	*S. lawsi*	5.7
S. demani	4.7							*S. punctata*	2.0	*S. ornata*	5.7
										S. punctata	4.3
										S. vasicola	2.9